09

Study of directional couplers for optical qubit quantum operations

© I.O. Venediktov,[1,2] V.V. Kovaluk,[1,3] P.P. An,[2,3] A.D. Golikov,[2] S.S. Svyatodukh,[1,2] G.N. Goltsman[1,4]

[1] National Research University „Higher School of Economics“,
109028 Moscow, Russia
[2] Moscow Pedagogical State University,
119991 Moscow, Russia
[3] National University of Science and Technology MISiS,
119049 Moscow, Russia
[4] Russian Quantum Center,
121205 Moscow, Russia
e-mail: ilia1999ven@gmail.com

Received May 3, 2023
Revised May 3, 2023
Accepted May 3, 2023

In this work, nanophotonic circuits with directional couplers are studied, which, along with phase shifters, are one of the main elements for creating circuits of a linear optical quantum computer. Directional couplers are two closely spaced waveguides, were made of silicon nitride. The subject of the study was the splitting ratio of directional couplers at a wavelength of 914 nm at room (300 K) and helium (3 K) temperatures. On the basis of experimental data, the coupling length at which all the power from one waveguide passes into another was extracted, and the refractive indices of silicon nitride at room (300 K) and helium temperatures (3 K) were found. The results of the work are of great importance in the design and manufacture of fully integrated quantum optical microcircuits with superconducting detectors operating at helium temperatures.

Keywords: photonic integrated circuits, directional coupler, silicon nitride, quantum optical integrated circuits, scalable photon quantum computer.

DOI: 10.61011/TP.2023.07.56636.80-23

Introduction

A quantum computer is able to solve certain classes of problems much faster, which have applications in cryptography, molecular analysis, mathematical data processing [1]. There are several approaches to the implementation of a quantum computer, differing in the physical implementation of qubits. Various physical objects in the superposition of two orthogonal states can be used as qubits. The use of photons is one of the most promising ways to implement qubits along with superconducting circuits, trapped ions and atoms [1]. Photons have a number of advantages over other platforms, including many degrees of freedom for encoding (frequency, phase, polarization, angular momentum, spatial distribution between waveguides), ease of implementing passive gates, high stability of the quantum state without interaction with matter [2]. The quantum gates can be implemented in the integrated optical design of a quantum computer in the form of beam splitters and phase shifters [3], and photon detection can be implemented using single-photon detectors [4]. The most promising detectors with record-breaking characteristics in the optical and telecommunication wavelength range are superconducting Single Photon detectors (Superconducting Single Photon Detectors, SSPDs), invented in Russia in 2001 g. [5]. Such detectors are already integrated with various photonic platforms, including SOI [6], GaAs [7], Si_3N_4 [8], polycrystalline diamond [9], LNOI [10] along with high detection efficiency ($> 85\%$), low dark sampling rate (< 10 Hz), high time resolution (< 50 ps). Since SSPDs operate at cryogenic temperatures, it is important to take into account the temperature dependence of the refractive index of both the waveguide material (core) and the environment (cladding) when designing dividers and phase shifters. A directional coupler is one of the simplest beam-splitting schemes. This device consists of two waveguides brought together at a close distance (on the order of the wavelength of radiation). The power flows from one waveguide to another due to the evanescent wave (near field). The division coefficient depends on the interaction length of the waveguides (L_i), at which the waveguides are brought close enough to each other, on the distance between the waveguides (L_g), on the refractive indices of the waveguide material (core and environment), as well as on the medium between them. Both the geometric parameters of the structure (due to the coefficient of linear expansion) and the refractive indices of the materials that make up the structure can change with a decrease in temperature. Such changes can greatly change the splitting ratio. The paper [11] shows the dependence of the splitting ratio of directional couplers from Si_3N_4 on the distance between the waveguides, this dependence is exponential, so even a small change in the geometry of the waveguides will lead to a large change in the division coefficient. In addition, the paper [11] provides the dependence of the transmission in one of the ports of the couplers on the wavelength, from which it

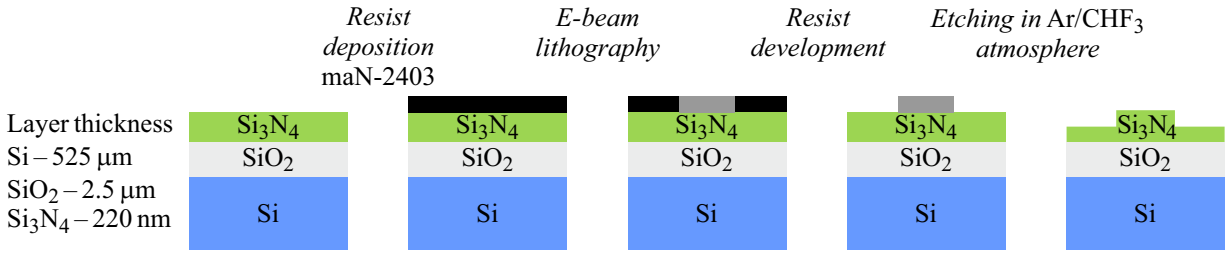

Figure 1. The scheme of the technological route, which includes the following main stages: application of the maN-2403 resist, electronic lithography, manifestation of the resist, plasma chemical etching in the atmosphere Ar/CHF_3.

can be seen that the wavelength also significantly affects the splitting ratio, which indicates a strong dependence of the splitting ratio on the refractive index of the waveguide material. Speaking about the temperature dependence of the refractive index Si_3N_4, most works show a change in the refractive index Si_3N_4 at temperatures above 300 K. Thus, the work [12] shows the dependence of the splitting ratio for curved directional couplers in the temperature range from 287 to 363 K, due to the geometry and the use of LPCVD Si_3N_4 the authors managed to achieve a reduction the temperature dependence of the splitting ratio by 85% compared to silicon structures, and also reduce the effect of wavelength on the splitting ratio. We studied in this paper the change of the splitting ratio of the directional coupler as a function of the interaction length at room (300 K) and helium (3 K) temperatures at a wavelength of 914nm

1. Device fabrication route

Commercially available plates made of stoichiometric LPCVD (Low pressure chemical vapor deposition) silicon nitride were used to manufacture nanophotonic devices. The thickness of the silicon substrate was 545 μm, the thickness of thermal oxide was SiO_2 2.5 μm and the thickness of Si_3N_4 was 225 nm. A negative resist (maN-2403) was applied at the first stage of manufacturing by centrifugation in which a resist thickness equal to 300 nm was formed for 60 s and 3400 r/s. After that, the resist was dried at a temperature of 90°C for 2 min, and electron lithography was performed at CABL 9050C (Centre for Collective Use of MIPT) with an accelerating voltage of 50 kV, a beam current of 150 pA and a dose of 80 $\mu C/cm^2$. Then the resist development was done in MF-319 for 60 s. At the second stage, plasma chemical etching was performed using Corial 200R system in an atmosphere of working gases: Ar and CHF_3. The etching rate was about 1 nm/s, was controlled by a reflectometer built into the installation, and the etching itself was performed at half the thickness of silicon nitride. The manufacturing process was completed by the stage of removing the electronic resist in a solution of N-methyl-2-pyrrolidone (NMP). The scheme of the manufacturing flow is shown in Fig. 1.

2. Description of the device

A typical device consisted of two closely spaced waveguides, each connected to two Focusing Grating Arrays (FGS) optimized for wavelength $\lambda = 925$ nm (Fig. 1). The wavelength was chosen for the possibility of further integration of the detector and the directional coupler with a single-photon source from a quantum dot based on GaAs [13]. The waveguides of the directional coupler were at a distance of 0.5 μm (gap) at length L_i („interaction site“ in Fig. 2), at which optical power flowed from one waveguide to another due to the evanescent field. The length of the interaction section from structure to structure varied from 16 to 100 μm with increments of 6 μm.

3. Modeling of directional couplers

We simulated the distribution of E_x components of the electromagnetic field in the cross section of the waveguides to determine the interaction length at which the optical power completely flows from one waveguide to another (Fig. 3, *a, b*). The numerical model used values for the refractive index [14,15] $n(SiO_2, 300K) = 1.4516$, $n(Si_3N_4, 300\,K) = 1.9908$, $n(\text{air}) = 1$, for silicon oxide, silicon nitride and air, respectively. The values of $n_{\text{eff},odd}$ and $n_{\text{eff},even}$ were obtained from the simulation for two modes propagating in waveguides: odd and even, respectively. The dependence of $n_{\text{eff},odd}$ and $n_{\text{eff},even}$ on the distance between the waveguides (Fig. 3, *c*) and the etching depth was calculated after that. The coupling length (L_C) was found using the obtained values of the effective refractive index showing at what interaction length of the interaction of waveguides there is a complete flow of power from one to the other.

The calculation of the coupling length (L_C) was performed using the formula

$$L_C = \lambda/(2|n_{\text{eff},odd} - n_{\text{eff},even}|), \quad (1)$$

where λ is the wavelength in vacuum. Fig. 4 shows the dependence of the coupling length on the etching depth of the waveguides and the distance between the waveguides. L_C increases with the increase of the distance between waveguides and etching depth, which can be explained by an increase of the area between waveguides with a lower

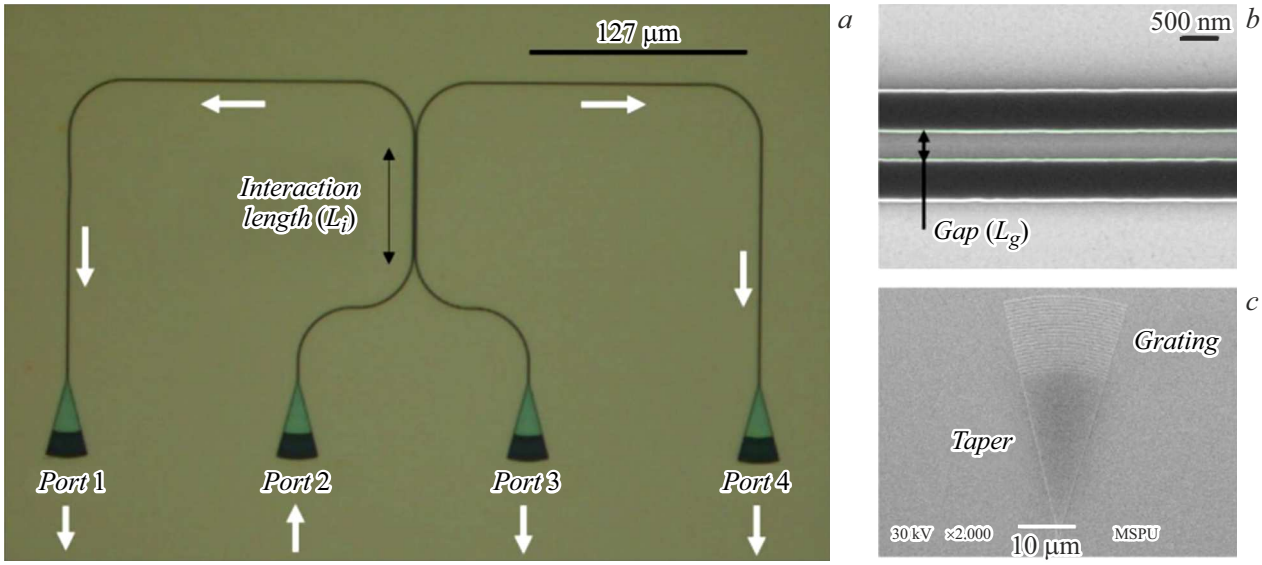

Figure 2. Micrograph of a directional coupler, including: *a* — general view of the structure, *b* — enlarged image of the central part of the directional coupler acquired using a scanning electron microscope (SEM), *c* — enlarged image of a focusing diffraction grating acquired using SEM.

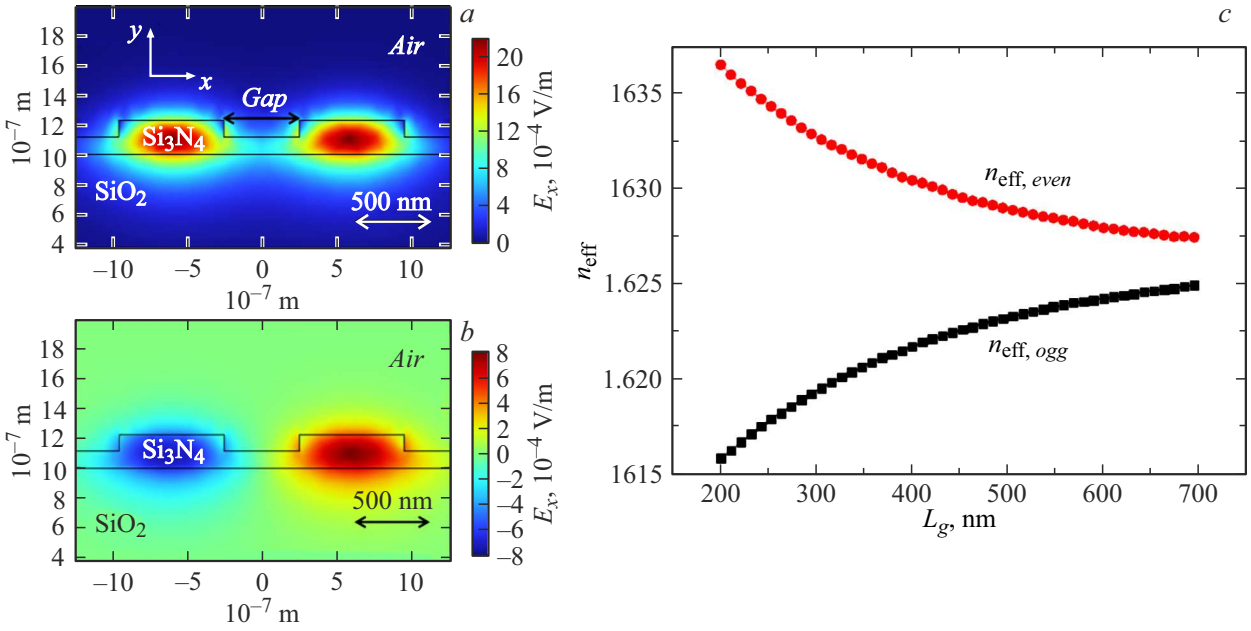

Figure 3. Distribution of the electric field E_x in the cross section of the directional coupler: *a* — for the even mode, *b* — for theodd mode of the directional coupler, *c* — dependence of the effective refractive index for even (red dots (in online version)) and odd (black dots) modes on the distance between the waveguides at $\lambda = 914$ nm and with the etching depth of $h_e = 110$ nm.

refractive index, which slows down the flow of power. The coupling length was $L_C = 80.18\,\mu$m with the etching depth of 110 nm and the distance between the waveguides of 500 nm.

4. Measurement procedure and results

At the first stage of the experiment, the chip with ready-made devices was located on a table with piezo positioners, which provided motion in the directions x, y, z , and rotated in the plane xy. The table was used to align the array of fibers relative to the focusing couplers on the chip, and the Peltier element with a PID controller stabilized the temperature of the chip at room temperature. The radiation was input and output using an array of fibers located above the nanophotonic chip at an angle of 8° to normal. The radiation was introduced into port 2 (Fig. 1) during measurements and the optical power coming out of

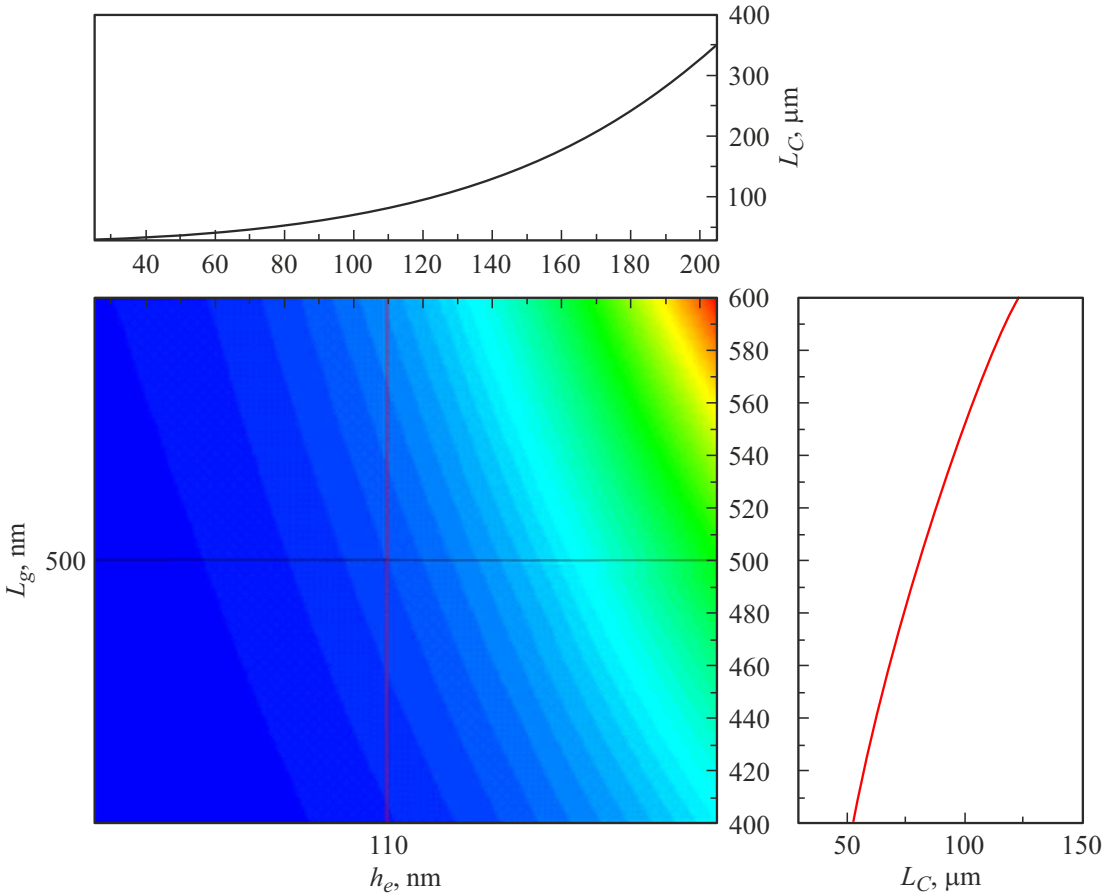

Figure 4. The dependence of the coupling length (L_C) on the wavelength $\lambda = 914$ nm on the distance between the waveguides (L_g) and the etching depth (h_e), found using the results numerical simulation of the even and odd modes of the directional coupler and formula (1).

the other ports was measured. Ports 1 and 4 were used to measure the splitting ratio directly, and the power value from port 3 — to estimate the reflection from the directional coupler, which amounted to about 4–5% of the total optical output power. At the second stage, the manufactured structures were measured at a temperature of 3 K in the original measurement setup based on the SRDK-101D closed-cycle machine using AttoCube cryogenic movements. The unit diagram is shown in Fig. 5.

The results of the splitting ratio measurements calculated using the division formula (2) for two measurement stages are shown in Fig. 6, where the red (in the online version) and black dots — are the measured values of the division coefficient at room and helium temperatures, respectively, and solid lines show the result of approximation by the cosine dependence

$$k = P_1/(P_1 + P_4), \tag{2}$$

where P_1 and P_4 — optical power in ports 1 and 4, respectively (Fig. 2). The data obtained were approximated using a cosine dependence of the form

$$k(L_i) = \big(1 + \cos(\pi L_i/L_C)\big)/2. \tag{3}$$

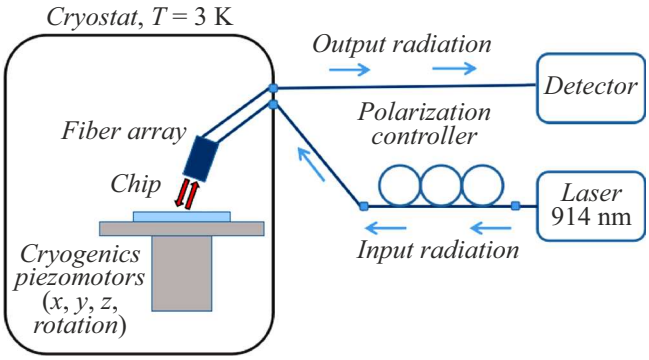

Figure 5. A experimental setup including a cryostat, cryogenic piezoelectric devices, an array of fibers, a laser source $\lambda = 914$ nm, a polarization controller and a fast photodetector.

The values of the characteristic coupling lengths $L_C = 79 \pm 0.87\,\mu$m and $71.3 \pm 1.24\,\mu$m were obtained as a result of approximation for room and cryogenic temperatures, respectively. The experimentally obtained value of L_C for room temperature is close to the numerical calculation of $80.18\,\mu$m. The decrease in the interaction

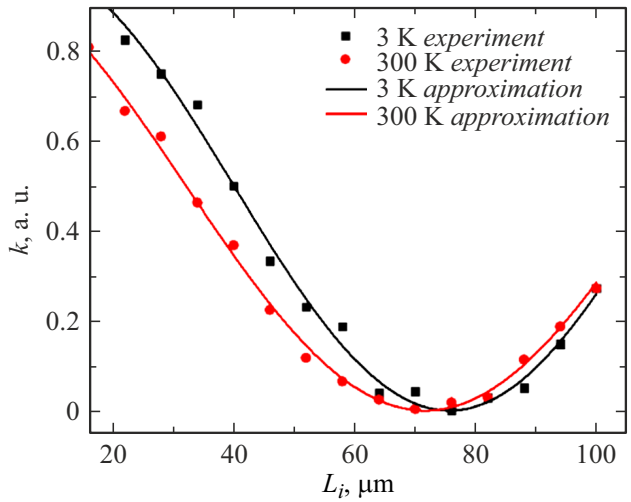

Figure 6. The results of measurements of the splitting ratio of directional couplers measured at room (300 K) and cryogenic (3 K) temperatures calculated by formula (2) and approximated using the formula (3).

length is associated with a decrease in the refractive index of both Si_3N_4 and SiO_2 with temperature. The authors were not able to find the refractive index values for the stoichiometric LPCVD Si_3N_4 at a temperature of 3 K used in our work in the literature data. The dependences of the thermo-optical coefficients for PECVD silicon nitride (Plasma-enhanced chemical vapor deposition) and thermal oxide SiO_2 are presented in [16]. However, the refractive index PECVD of silicon nitride, as well as its thermo-optical coefficient, may differ greatly from the stoichiometric LPCVD Si_3N_4, therefore it can only be used as a rough estimate. Using the data on the thermo-optical coefficient from [16] together with the values of the refractive indices $n(\mathrm{SiN},\ 3\,\mathrm{K}) = 2.022$, $n(\mathrm{SiN}, 300\,\mathrm{K}) = 2.0259$, $n(SiO_2,\ 3\,\mathrm{K}) = 1.4501$, $n(SiO_2,\ 300\,\mathrm{K}) = 1.4516$, and the numerical calculation method described above, we first found the change in bond length from temperature for PECVD silicon nitride (Fig. 7, *b*). It can be seen that the coupling length (as well as in our experiment) decreases with the decrease of the temperature, but much less than we observed (1.3% instead of 10.1% in our case). Qualitatively, the decrease of L_C is associated with an increase in the diameter of the mode in the waveguide, as a result of which a large power of the evanescent wave reaches the neighboring waveguide, flowing into it faster. We associate the quantitative difference with the different refractive index values for PECVD and LPCVD silicon nitride at both room and helium temperatures. Using $n(SiO_2,\ 3\,\mathrm{K}) = 1.4501$ [16], we varied the refractive index for silicon nitride, achieving a coincidence of the measured coupling length with the experimental $L_C = 71.3 \pm 1.24\,\mu$m (Fig. 7, *a*) and obtained an estimate $n(Si_3N_4,\ 3\,\mathrm{K}) = 1.953$ by $\lambda = 914$ nm.

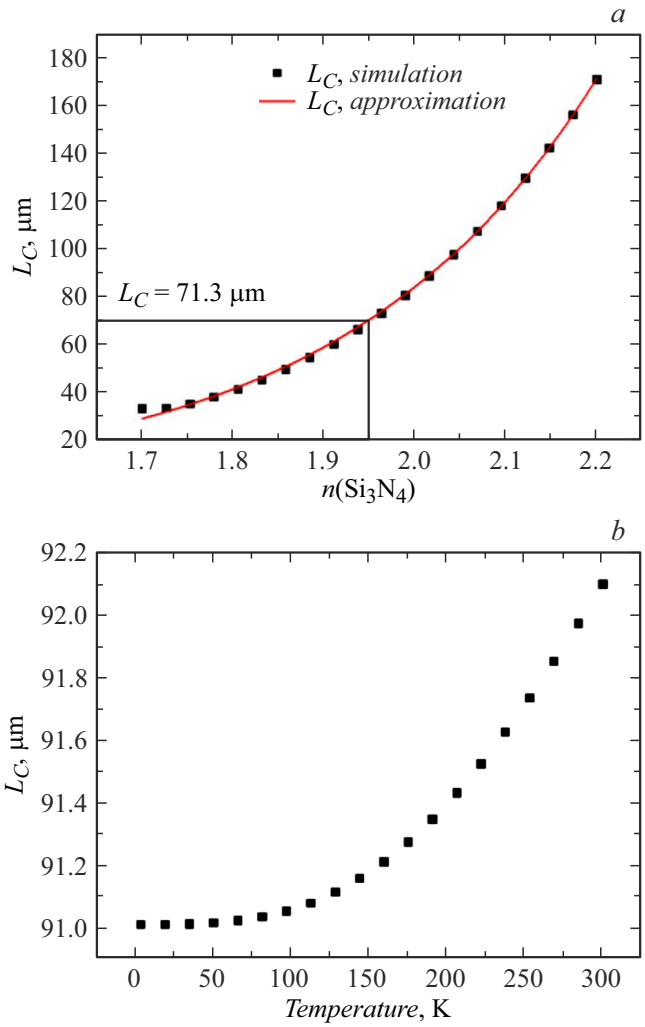

Figure 7. *a* — dependence of the coupling length with a fixed value $n(SiO_2,\ 3\,\mathrm{K}) = 1.4501$ [14] and a variable value of the refractive index $n(Si_3N_4,\ 3\,\mathrm{K})$ in the range 1.7–2.2. The arrow indicates a value consistent with the experimentally obtained data $L_C = 71.3 \pm 1.24\,\mu$m; *b* — numerically calculated dependence of the coupling length on temperature for PECVD silicon nitride according to [16].

Conclusion

The splitting ratio of directional couplers made of silicon nitride was measured in the paper. The dependences of the splitting ratio on the interaction length of the waveguides were measured, and the coupling lengths $L_C = 79 \pm 0.87\,\mu$m and $71.3 \pm 1.24\,\mu$m were found for room (300 K) and cryogenic (3 K) temperatures, respectively. Qualitatively, we associate a decrease in L_C with a decrease in temperature with a decrease in the refractive index of both Si_3N_4 and SiO_2. This increases the volume of the optical mode in the waveguide and the power of the evanescent wave reaching the adjacent waveguide. The refractive index used by us in the work of stoichiometric Si_3N_4 at a temperature of 3 K was obtained, which was

$n(Si_3N_4,\ 3\,K) = 1.953$ at $\lambda = 914\,nm$ was obtained based on experimental data. The obtained data can be used in the design and manufacture of scalable quantum-optical integrated circuits with superconducting single-photon detectors operating at cryogenic temperatures and implementing operations on optical qubits.

Funding

This study was supported by „Rosatom“ as part of the Quantum Computing Roadmap (Contract №868-1.3-15/15-2021 of 05.10.2021 and Contracts №P2178, P2179).

Conflict of interest

The authors declare that they have no conflict of interest.

References

[1] T.D. Ladd, F. Jelezko, R. Laflamme, Y. Nakamura, C. Monroe, J.L. O'Brien. Nature, **464**, 45 (2010). DOI: 10.1038/nature08812
[2] H.S. Zhong, Hui Wang, Yu-Hao Deng, Ming-Cheng Chen, Li-Chao Peng, Yi-Han Luo, Jian Qin, Dian Wu, Xing Ding, Yi Hu, Peng Hu, Xiao-Yan Yang, Wei-Jun Zhang, Hao Li, Yuxuan Li, Xiao Jiang, Lin Gan, Guangwen Yang, Lixing You, Zhen Wang, Li Li, Nai-Le Liu, Chao-Yang Lu, Jian-Wei Pan. Science, **370**, 1460 (2020). DOI: 10.1126/science.abe8770
[3] E. Knill, R. Laflamme, G.J. Milburn. Nature, **409**, 46 (2001). DOI: 10.1038/35051009
[4] J.L. O'Brien, G.J. Pryde, A.G. White, T.C. Ralph, D. Branning. Nature, **426**, 264 (2003). DOI: 10.1038/nature02054
[5] G.N. Gol'tsman, O. Okunev, G. Chulkova, A. Lipatov, A. Semenov, K. Smirnov, B. Voronov, A. Dzardanov. Appl. Phys. Lett., **79** (6), 705 (2001). DOI: 10.1063/1.1388868
[6] W.H.P. Pernice, C. Schuck, O. Minaeva, M. Li, G.N. Goltsman, A.V. Sergienko, H.X. Tang. Nat. Commun., **3**, 1325 (2012). DOI: 10.1038/ncomms2307
[7] J.P. Sprengers, A. Gaggero, D. Sahin, S. Jahanmirinejad, G. Frucci, F. Mattioli, R. Leoni, J. Beetz, M. Lermer, M. Kamp, S. Hfling, R. Sanjines, A. Fiore. Appl. Phys. Lett., **99**, 181110 (2011). DOI: 10.1063/1.3657518
[8] O. Kahl, S. Ferrari, V. Kovalyuk, G.N. Goltsman, A. Korneev, W.H.P. Pernice. Sci. Rep., **5**, 10941 (2015). DOI: 10.1038/srep1094
[9] P. Rath, O. Kahl, S. Ferrari, F. Sproll, G. Lewes-Malandrakis, D. Brink, K. Ilin, M. Siegel, C. Nebel, W. Pernice. Light Sci. Appl., **4**, e338 (2015). DOI: 10.1038/lsa.2015.111
[10] A. Al Sayem, R. Cheng, S. Wang, H.X. Tang. Appl. Phys. Lett., **116**, 151102 (2020). DOI: 10.1063/1.5142852
[11] A. Prokhodtsov, V. Kovalyuk, P. An, A. Golikov, R. Shakhovoy, V. Sharoglazova, A. Udaltsov, Y. Kurochkin, G. Goltsman. J. Phys. Conf. Series, **1695** (1), 012118 (2020). DOI: 10.1088/1742-6596/1695/1/012118
[12] L. Donghao, L. Bin, T. Bo, Z. Peng, Y. YanL. Ruonan, X. Ling, L. Zhihua. Micromachines, **13** (4), 559 (2022). DOI: 10.3390/mi13040559
[13] A.I. Galimov, M.V. Rakhlin, G.V. Klimko, Yu.M. Zadiranov, Yu.A. Guseva, S.I. Troshkov, T.V. Shubina, A.A. Toropov. JETP Lett., **113** (4), 252 (2021). DOI: 10.31857/S1234567821040054
[14] K. Luke, Y. Okawachi, M.R.E. Lamont, A.L. Gaeta, M. Lipson. Opt. Lett., **40**, 4823 (2015).
[15] I.H. Malitson. J. Opt. Soc. Am., **55**, 1205 (1965).
[16] A.W. Elshaari, I.E. Zadeh, K.D. Jöns, V. Zwiller. IEEE Photon. J., **8**, 1 (2016). DOI: 10.1109/JPHOT.2016.2561622

Translated by A.Akhtyamov